AFRL-RY-WP-TP-2013-0024

MODULATION EFFECTS IN MULTI-SECTION SEMICONDUCTOR LASERS (POSTPRINT)

Nicholas G. Usechak, Matt Grupen, and Vassilios Kovanis

Optoelectronic Technology Branch
Aerospace Components & Subsystems Division

Nader Naderi, Yan Li, and Luke F. Lester

University of New Mexico

JANUARY 2013
Interim

AIR FORCE RESEARCH LABORATORY
SENSORS DIRECTORATE
WRIGHT-PATTERSON AIR FORCE BASE, OH 45433-7320
AIR FORCE MATERIEL COMMAND
UNITED STATES AIR FORCE

REPORT DOCUMENTATION PAGE

Form Approved
OMB No. 0704-0188

1. REPORT DATE *(DD-MM-YY)*	2. REPORT TYPE	3. DATES COVERED *(From - To)*
January 2013	Technical Paper	15 September2008 – 16 February 2011

4. TITLE AND SUBTITLE
MODULATION EFFECTS IN MULTI-SECTION SEMICONDUCTOR LASERS (POSTPRINT)

5a. CONTRACT NUMBER
In-house

5b. GRANT NUMBER

5c. PROGRAM ELEMENT NUMBER
61102F

6. AUTHOR(S)
Nicholas G. Usechak, Matt Grupen, and Vassilios Kovanis (AFRL/RYDH)
Nader Naderi, Yan Li, and Luke F. Lester (University of New Mexico)

5d. PROJECT NUMBER
2305

5e. TASK NUMBER
DP

5f. WORK UNIT NUMBER
Y05T

7. PERFORMING ORGANIZATION NAME(S) AND ADDRESS(ES)
Optoelectronic Technology Branch
Aerospace Components & Subsystems Division
Air Force Research Laboratory, Sensors Directorate
Wright-Patterson Air Force Base, OH 45433-7320
Air Force Materiel Command, United States Air Force

University of New Mexico

8. PERFORMING ORGANIZATION REPORT NUMBER
AFRL-RY-WP-TP-2013-0024

9. SPONSORING/MONITORING AGENCY NAME(S) AND ADDRESS(ES)
Air Force Research Laboratory, Sensors Directorate
Wright-Patterson Air Force Base, OH 45433-7320
Air Force Materiel Command
United States Air Force

Air Force Office of Scientific Research (AFOSR)

10. SPONSORING/MONITORING AGENCY ACRONYM(S)
AFRL/RYDH

11. SPONSORING/MONITORING AGENCY REPORT NUMBER(S)
AFRL-RY-WP-TP-2013-0024

12. DISTRIBUTION/AVAILABILITY STATEMENT
Approved for public release; distribution unlimited.

13. SUPPLEMENTARY NOTES
Journal article published in SPIE Proceedings Vol. 7933 ©2011 SPIE. The U.S. Government is joint author of the work and has the right to use, modify, reproduce, release, perform, display or disclose the work. PAO Case Number 88ABW-2011-0247, Clearance Date 21 January 2011. Report contains color.

14. ABSTRACT
The current modulation of a two-section semiconductor laser is first reviewed analytically using a well-known, closed-form, modulation expression. A system of traveling-intensity equations is then used to investigate spatial effects in these lasers including cavity layout and the role played by cavity length. The numerical simulations verify the accuracy of the analytic expression for short cavities (low frequencies) but identify shortcomings as the cavity length (modulation frequency) is increased. One notable difference is the presence of resonant peaks in the modulation response. Although this effect has been addressed in the past, the arrangement of sections within the laser is shown to play a prominent role in these monolithic devices for what we believe to be the first time. In the course of this investigation the thirteen different ways a two-section semiconductor laser can be current modulated are identified and computationally investigated.

15. SUBJECT TERMS
Multi-section semiconductor lasers, laser modulation, RF photonics, gain lever, feedback-enhanced modulation, resonant modulation

16. SECURITY CLASSIFICATION OF:			17. LIMITATION OF ABSTRACT:	18. NUMBER OF PAGES	19a. NAME OF RESPONSIBLE PERSON (Monitor)
a. REPORT	b. ABSTRACT	c. THIS PAGE			Nicholas Usechak
Unclassified	Unclassified	Unclassified	SAR	14	19b. TELEPHONE NUMBER *(Include Area Code)* N/A

Invited Paper

Modulation effects in multi-section semiconductor lasers

Nicholas G. Usechak[a], Matt Grupen[a], Nader Naderi[b], Yan Li[b],
Luke F. Lester[b], and Vassilios Kovanis[a]
[a]Air Force Research Laboratory, 2241 Avionics Circle, Wright–Patterson AFB, OH 45433, USA
[b]Center for High Technology Materials, University of New Mexico,
1313 Goddard SE, Albuquerque, NM 87106, USA

ABSTRACT

The current modulation of a two-section semiconductor laser is first reviewed analytically using a well-known, closed-form, modulation expression. A system of traveling-intensity equations is then used to investigate spatial effects in these lasers including cavity layout and the role played by cavity length. The numerical simulations verify the accuracy of the analytic expression for short cavities (low frequencies) but identify shortcomings as the cavity length (modulation frequency) is increased. One notable difference is the presence of resonant peaks in the modulation response. Although this effect has been addressed in the past, the arrangement of sections within the laser is shown to play a prominent role in these monolithic devices for what we believe to be the first time. In the course of this investigation the thirteen different ways a two-section semiconductor laser can be current modulated are identified and computationally investigated.

Keywords: Multi-section semiconductor lasers, laser modulation, RF photonics, gain lever, feedback-enhanced modulation, resonant modulation

1. INTRODUCTION

The modulation of semiconductor lasers has been investigated since the 1960s when they were first* placed inside microwave waveguides to achieve optical modulation at RF frequencies [1]. In spite of its long history, laser modulation is more relevant today than ever for applications such as antenna remoting, clock distribution, communications, and as an experimental tool to extract laser parameters such as lifetimes. Still, the majority of research performed in this area has focused on the uniform modulation of the entire laser cavity. This is no surprise since these devices are easily made, readily available, and consequently the most heavily studied.

Although the modulation of single-section lasers has received considerable attention, multi-section lasers have an equally long history dating back to Lasher's proposal of a bistable laser for use as a high-speed optical element in 1964 [2]. Indeed, this topology was experimentally investigated directly following its proposal [3-5], although threshold could only be reached under pulsed operation at the time. Initial investigations focused on a situation where one of the sections was exploited for its saturable absorption properties which promoted bi-stability [5] or the formation of transient pulses [6]. This work spurred investigations into Q-switching (see [7] and the references therein) and coincided with the demonstration of the first passively mode-locked semiconductor laser [8]. It is interesting to note that in Ref. [8] an external cavity was used to achieve mode locking; a monolithic mode-locked semiconductor laser was not realized until decades later [9] despite the contemporary device topology being essentially the same as that proposed in Ref. [2].

In the context of the present work, where we are concerned with the role of optical feedback on laser modulation, it is important to point out a somewhat separate community, more aligned with injection-locked lasers, which considered the role of semiconductor lasers in free-space external Fabry–Perot cavities [10-15]. The mode locking of such lasers [8, 11] was first investigated analytically using a rate-equation model in the late 1970's [16, 17]. Ultimately,

*In this work we are focusing on cw sinusoidal modulation. Earlier pulsed modulation work was done by Goldstein and others.

Physics and Simulation of Optoelectronic Devices XIX, edited by Bernd Witzigmann,
Fritz Henneberger, Yasuhiko Arakawa, Alexandre Freundlich, Proc. of SPIE Vol. 7933,
79331I · © 2011 SPIE · CCC code: 0277-786X/11/$18 · doi: 10.1117/12.876513

the small-signal modulation response of these lasers was investigated both analytically and experimentally by Glasser [18]. Indeed, in Ref. [18] cavity effects, as they pertain to small-signal modulation, were studied analytically for the first time. Specifically, the role of cavity/feedback enhancement, also referred to as "resonant modulation", was investigated using a delay model which sought to include the external cavity's periodic boundary condition while still treating the laser as a point source within this larger free-space cavity. By exploiting the enhancement offered by a heterogeneously modulated cavity, very high-frequency modulation, beyond that available due to carrier-relaxation dynamics, was later achieved at the expense of modulation bandwidth [19]. To conceptually understand this feedback-enhanced modulation we note that the small-signal modulation of a longitudinally heterogeneous semiconductor laser at an integer multiple of the cavity's free-spectral range [FSR = $c/(2nl)$] can be visualized as sub-threshold AM mode locking where the applied current is assumed to be weak and the optical output is therefore still sinusoidal.

Despite Glasser's theory, most analytic investigations into the small-signal modulation of external-cavity semiconductor lasers only considered modulation below the FSR of the cavity [20, 21] and therefore did not address these feedback-enhanced peaks in greater detail. This effect, however, did not go unnoticed experimentally as it was heavily exploited by Lau *et al*. to increase the modulation frequency of a semiconductor laser from a record modulation of 10 GHz in 1984 (without this effect) [22] to $>$ 17 GHz the following year [19] and then to $\sim$ 70 GHz only a few years later [23-25]. In the late 1980's and early 1990's, studying the deleterious effects of weak, yet generally unwanted, "back" reflections from e.g. optical fibers became industrially relevant and spurred renewed theoretical interest in this effect. Accordingly, feedback from small external cavities on the modulation behavior of semiconductor lasers was studied with greater interest [26-28].

Although the work performed in Refs. [26-28] is directly relevant to the present endeavor, these former efforts considered only the feedback from a long passive cavity on, what was in contrast, a short semiconductor laser. As the round-trip times between the semiconductor laser and the external cavity easily differed by an order of magnitude or more, treating the semiconductor laser as a point source buried in a larger Fabry–Perot cavity (as in [18]) was still a good approximation. In this paper, however, this approximation breaks down because the effects of feedback within a two-section semiconductor laser are addressed. In this case[†], there is no passive feedback section (as the entire cavity is formed by active semiconductor) and the spatial dimension of the semiconductor must be accounted for explicitly in any model or theory as the photon density can no longer be considered constant over the cavity length.

Despite the early work done on multi-section lasers in the late 1960's by Lasher, Nathan, Basov, and others [2, 5, 6], the later work on monolithic mode-locked lasers starting with Ref. [9], and modulation studies performed on two mutually coupled semiconductor lasers [29], the value of modulating a multi-section semiconductor laser was not fully exploited until Vahala *et al*. demonstrated the beneficial modulation properties of two-section lasers in 1989 [30]. Here an effect, termed the "gain lever", improves the modulation efficiency and allows the 3-dB modulation bandwidth to be extended to higher frequencies by partitioning a laser into two sections, each biased above threshold but at different levels, of which only one is modulated [30-32]. As a consequence of the bandwidth enhancement and other beneficial characteristics offered by this approach, it has been the focus of over a hundred studies including Refs. [32-46] and is still attracting interest today as higher bandwidths are sought and new gain platforms explored [47].

In the present work, a brief review of the principal findings governing the modulation of a two-section semiconductor laser is presented [31, 47]. Then spatial effects in these lasers and their computer simulations are described. By using a system of partial differential equations, the gap between the spatially agnostic gain-lever and external-cavity feedback lasers is bridged, since both structures can be represented under this single model. While others have used models more complex than that presented here to study the gain-lever effect [41, 44], their attention was primarily restricted to modulation well below the laser's FSR, with few exceptions [46]. As a consequence, neither the resonant modulation of these devices nor the role played by the placement of sections within the laser cavity has been fully explored. These two issues have become important as long-cavity multi-section semiconductor lasers have recently been demonstrated [48, 49]. In particular, the inherent reconfigurability of this new breed of laser, which allows one to electronically change the cavity layout extemporaneously, requires a more thorough investigation into these effects. Experimental findings, numerical predictions, and a new analytic theory will be published elsewhere.

[†]Sub-cavity effects are assumed to play no role in the present work.

2. THE GAIN-LEVER EFFECT

In 1989 Vahala *et al.* coined the term "gain lever" to describe a modulation scheme which exploited the advantageous properties intrinsic to a segmented two-section semiconductor laser under asymmetric pump levels [30]. This scheme was immediately investigated with an analytic model [31] using a system of well-known rate equations [6]. The effect can be summarized by noting that biasing one section at a lower current (relative to the other section) results in an increased differential gain in that section. The increased differential gain enables optical [30] or electrical [31] modulation to be more efficiently converted to the laser's output. Figure 1 pictorially depicts a two-section laser while also highlighting this effect. A gain verses carrier density curve is provided in Fig. 1 to explain the improved differential gain available at lower carrier bias levels which can be seen by the difference in the differential gains, shown here as the slopes G'_b and G'_m.

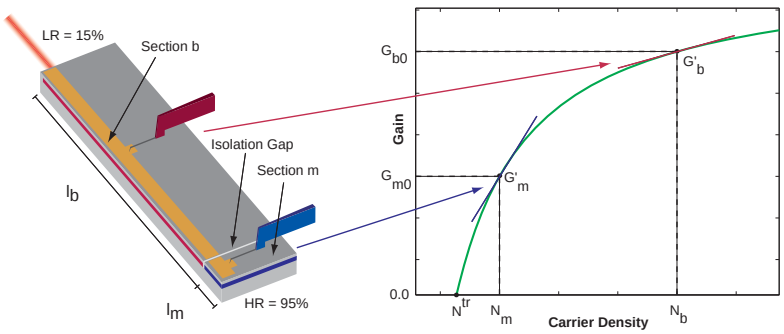

Fig. 1. Depiction of a two-section semiconductor laser (left). The laser is partitioned into a section under a constant current bias "Section b" and a section which is biased at a constant current but also modulated "Section m". The lengths of the biased and modulated sections are denoted by l_b and l_m respectively while the overall device length $L = l_b + l_m$ is not shown. Probe contacts depicted in red and blue identify how these devices are frequently addressed in a research environment but are not part of the device. The facet reflectivity's are assumed to be highly asymmetric and denoted by HR: high reflectivity and LR: low reflectivity. The gain verses carrier density curve (right) clearly identifies the higher differential gain (G'_m) at lower current densities (N_m) in comparison to that (G'_b) available at higher current densities (N_b). The commonly used transparency gain N^{tr} has also been included in this figure because of its role in Eqs. (13) and (14) introduced in the next section.

The rate-equation model typically used to investigate the gain lever [47] originates from a long-standing system of equations which govern the photon density and the carrier concentrations in each of the two sections [2] and is generally written in the form [47]:

$$\frac{dS(t)}{dt} = \left[\Gamma G_m(N_m(t))(1-h) + \Gamma G_b(N_b(t))h - \frac{1}{\tau_p}\right] S(t), \tag{1}$$

$$\frac{dN_m(t)}{dt} = \frac{J_m(t)}{ed} - \frac{N_m(t)}{\tau_m} - G_m(N_m(t))S(t), \tag{2}$$

$$\frac{dN_b(t)}{dt} = \frac{J_b}{ed} - \frac{N_b(t)}{\tau_b} - G_b(N_b(t))S(t), \tag{3}$$

where we have followed [31] by using $l_m = (1-h)L$ and $l_b = hL$, L being the total cavity length.

Performing a linear stability analysis on this system of equations about its steady state and normalizing by the zero-frequency result gives the normalized modulation transfer function

$$H_{\text{norm}}(\omega) = \frac{A_2(\frac{i\omega}{\gamma_b}+1)}{-i\omega^3 - (\gamma_m+\gamma_b)\omega^2 + i\omega A_1 + A_2}, \tag{4}$$

where a linear gain assumption was used in this derivation [50]

$$G_{m,b}(N_{m,b}(t)) = G_{m0,b0} + G'_{m,b}(N_{m,b}(t) - N_{m0,b0}), \tag{5}$$

and

$$A_1 = \Gamma S_0 \left[G_{m0} G'_m (1-h) + G_{b0} G'_{b0} h \right] + \gamma_m \gamma_b, \tag{6}$$

$$A_2 = \Gamma S_0 \left[G_{m0} G'_m \gamma_b (1-h) + G_{b0} G'_{b0} \gamma_m h \right], \tag{7}$$

were introduced to simplify the appearance of the result. Finally, the damping rates of the modulated (γ_m) and biased (γ_b) sections are given by

$$\gamma_m = G'_m S_0 + \frac{1}{\tau_m} \tag{8}$$

$$\gamma_b = G'_b S_0 + \frac{1}{\tau_b} \tag{9}$$

respectively. Restricting our attention to the amplitude of the modulation response the result can be further simplified to

$$|H_{\text{norm}}(\omega)| = \frac{A_2 \sqrt{1 + \omega^2/\gamma_b^2}}{\sqrt{\omega^6 + \omega^4 B_1 + \omega^2 B_2 + A_2^2}}, \tag{10}$$

where the additional terms

$$B_1 = (\gamma_m + \gamma_b)^2 - 2A_1 \tag{11}$$

$$B_2 = A_1^2 - 2A_2(\gamma_m + \gamma_b) \tag{12}$$

have been introduced to highlight the functional dependence on frequency.

In Fig. 2 the predicted results for the modulation of a standard single-section laser [50], identical in form to a driven damped harmonic oscillator, are compared to those predicted from Eq. (10) for the gain lever. This figure clearly demonstrates that while both models predict the so-called primary resonance peak, the gain lever's added degrees of freedom (section length and the ability to independently select its bias point) enable the engineering of the modulation response. Still the gain-lever model states no preference for whether the modulated section is located adjacent to the output facet or at the other side of the cavity; this geometrical issue is taken up in the next section. Since we restricted our focus to only normalized modulation responses, the improved modulation efficiency at lower frequencies is not captured in Fig. 2, although it is of considerable practical utility [30].

3. TRAVELING INTENSITY EQUATIONS

Since the primary focus of this study was to investigate the role of cavity feedback and device geometry on laser modulation, a traveling-intensity equation model was used as the basis for our computational work [51]. This simplified variant of the more common (and rigorous) traveling-wave model [52] was chosen because it can be thought of as an only slightly more intelligent version of the traditional rate-equations used to model the gain-lever [47]. Despite its simplicity, this model can even be used to investigate transient effects such as Q-switching [51] or mode locking (albeit it constitutes a poor model for mode locking) making it sufficient to capture the effects currently under investigation. To avoid any confusion that would arise when comparing the two models, realistic effects frequently included in traveling-wave/intensity models (e.g. carrier heating, gain compression, and spectral filtering) have been omitted. Therefore, the model used here is essentially that of Eqs. (1) – (3) with the spatial dimension added:

$$\pm \frac{\partial I^{\pm}(t,z)}{\partial z} = -\frac{1}{v} \frac{\partial I^{\pm}(t,z)}{\partial t} + \Gamma g(z) \left[N(t,z) - N(z)^{\text{tr}} \right] I^{\pm}(t,z) - \alpha(z) I^{\pm}(t,z) + \beta B N(t,z)^2, \tag{13}$$

$$\frac{\partial N(t,z)}{\partial t} = \frac{J(t,z)}{ed} - \frac{N(t,z)}{\tau(z)} - B N(t,z)^2 - v g(z) \left[N(t,z) - N(z)^{\text{tr}} \right] \left[I^+(t,z) + I^-(t,z) \right]. \tag{14}$$

Equation (13) governs two counter-propagating intensity distributions under the slowly varying envelope approximation. This equation includes the optical confinement factor Γ, the group velocity v, a gain term g, and waveguide and

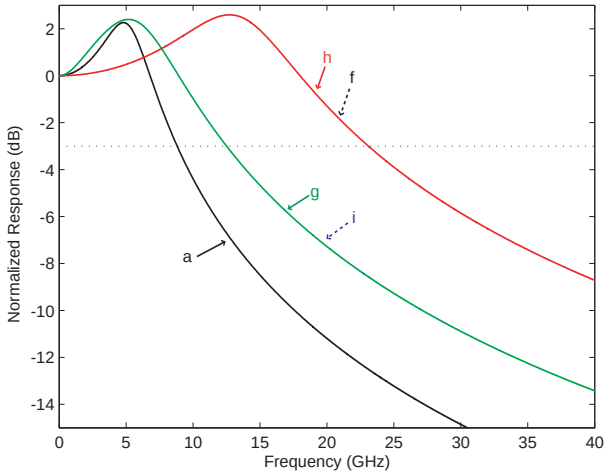

Fig. 2. Predicted modulation response from a single-section semiconductor laser (a) and two simple gain-lever configurations with identical properties except where necessary (f,h) and (g,i). Here the length of the two sections has been changed and the bias point and differential gain varied. The traces have been alphabetically labeled in accordance with the legend from Fig. 3 to depict the laser configurations they represent, although the numbers used to generate this figure were not extracted from the simulations presented later in this paper.

scattering losses α. These terms are allowed to vary along the cavity length allowing this model to easily investigate devices with an arbitrary number of sections and/or the placement of these sections within the cavity. Equation (14) governs the carrier density as a function of time and location within the laser cavity. Here a location-dependent current source J, relaxation term τ, and depletion term due to stimulated emission g have been included. A weak but deterministic noise term B has been added to both equations to coax the numerical solution to converge quickly, although its presence was confirmed to play no physical role in the results because of the values chosen.

Since Eqs. (1) – (3) can be derived from Eqs. (13) – (14) by spatially averaging over the cavity, the two models can easily be compared to one another. This provides the relationships between the rate-equation model (left-hand side) and the traveling-intensity model (right-hand side):

$$\frac{1}{\tau_p} = v\left[\alpha - \frac{1}{2L}\ln\left(R_{\text{left}}R_{\text{right}}\right)\right], \tag{15}$$

$$S(t) = \frac{1}{L}\int_0^L \left[I^+(t,z) + I^-(t,z)\right] dz, \tag{16}$$

$$N_m(t) = \frac{1}{\mathrm{l_m}}\int_0^{\mathrm{l_m}} N(t,z)dz, \tag{17}$$

$$N_b(t) = \frac{1}{\mathrm{l_b}}\int_{\mathrm{l_m}}^L N(t,z)dz, \tag{18}$$

$$G_{m,b}(t) = v g_{m,b}\left[N_{m,b}(t) - N^{\text{tr}}\right], \tag{19}$$

$$G'_{m,b} = v g_{m,b}, \tag{20}$$

$$g_m = v g(z) \text{ where } 0 < \mathrm{z} < \mathrm{l_m}, \tag{21}$$

$$g_b = v g(z) \text{ where } \mathrm{l_m} < \mathrm{z} < \mathrm{L}, \tag{22}$$

$$J_m(t) = J(t,z) \text{ where } 0 < \mathrm{z} < \mathrm{l_m}, \tag{23}$$

$$J_b = J(t,z) \text{ where } \mathrm{l_m} < \mathrm{z} < \mathrm{L}, \tag{24}$$

$$0 = B. \tag{25}$$

The terms S_0, $N_{m0,b0}$, and $G_{m0,b0}$ in Eqs. (4)–(12) are simply given by Eqs. (16)–(19) when the system has reached a steady state. Because $S(t) \neq I^+(t, z = L)$ but is related to the photon density averaged over the cavity, as given by Eq. (16), the extraction of experimental parameters using Eq. (1)–(3) is not as straightforward as one may expect or hope. Of course this is most problematic for cavities with asymmetric facet reflectivity's.

To model the two-section lasers investigated herein Eqs. (13) and (14) were solved by discretizing the cavity into as many as 500 sections of equal length. The resulting equations were then discretized using a robust higher-order spatial scheme [53] in conjunction with an implicit finite-volume method and solved self consistently with the Newton–Raphson method using a 500-fs temporal step size [54]. Although the modulation response can be extracted quickly by using a Fourier-transform based technique [54], a more time-consuming approach was used to verify the output always remained sinusoidal. By adding a weak sinusoidally varying signal to one section's bias current, the modulation behavior could then be extracted. To accomplish this the output was stored over a number of modulation cycles and fit with a sinusoid to extract the modulation depth and verify that the output waveform was still sinusoidal (i.e. the laser output was neither mode locked nor otherwise nonlinearly enhanced). This approach, which mirrors the way these curves are obtained experimentally, is repeated using a sinusoidal signal at a different frequency until the frequency range of interest has been swept at the required density.

4. NUMERICAL RESULTS

In this section, numerical simulations of Eqs. (13) and (14) are presented using realistic values consistent with quantum-well lasers. Specific focus is given to investigating the role played by the spatial location of the sub-cavity elements, and it is found, due to the asymmetric mirror reflectivity's, the length of the laser cavity, and the high modulation frequencies explored, that geometrical effects can play a prominent role in the modulation response even at frequencies well separated from the laser's FSR. We first consider a semiconductor laser of conventional length (400 μm) the results of which are shown in Fig. 3. In both Figs. 3 and 4, isolated sections with sinusoidal driving currents of varying frequencies have been applied to one or both sections as identified by the schematic insets in Fig. 3 (top right). The different traces in each figure come from varying which section is modulated, its location within the laser, and through changing the biasing conditions as identified in the legend of Fig. 3 (bottom left).

In Fig. 3, a 400-μm two-section laser is investigated computationally under nine different configurations. The figure clearly reveals three families of curves which highlight the gain-lever effect. Since the FSR of this cavity is $\sim$100 GHz, spatial effects were not found to play a prominent role in the modulation response of this device at the frequencies investigated and, as a consequence, all the results coalesced to those predicted by the gain-lever model of Eq. (10). These findings indicate that for lasers of similar lengths and modulation frequencies the existing theory is sufficient to explain experimental findings, at least as far as the role of spatial effects are concerned.

In Fig. 4, a 1.25-mm laser has been modeled and the frequency range extended. All the parameters used in the simulation of this longer cavity were identical to those used in Fig. 3 except the cavity length. Since the photon lifetime, τ_p, depends on the cavity length [see Eq. (15)] the primary resonance peaks are expected to shift; a result borne out by comparing the two figures closely. To avoid this discrepancy, it was verified that by changing the values of the facet reflectivity's for one of the two structures, to maintain a constant photon lifetime in both simulations, we obtained the same primary resonant peaks for both lasers. Nevertheless, Figs. 3 and 4 are sufficient to demonstrate the importance of the cavity length and did not make use of augmented reflectivities but both used those listed in Fig. 1.

Although carrier effects, capacitances, changes in the refractive index, or other phase effects, none of which are included in this model, could thwart the experimental realization of these exact results over the entire region depicted, this figure captures the role played by feedback in a longer structure. The striking resonant peaks, clearly visible above 30, 60, and 90 GHz are anticipated by both theory and experiment [18, 19, 27, 28] although the seemingly anomalous dips appearing at a number of frequencies were not commented on in the past to the best of our knowledge. The peaks, located at integer multiples of the laser's FSR ($\mathrm{FSR_{laser}}$), are the hallmark of cavity enhancement [18] and are due to photons synchronously passing through the modulated section over multiple round trips. This causes the modulation effect to accrue over time and enhances the modulation response at these frequencies. The width of these peaks is related to the finesse of the cavity and therefore limited by the high losses. In this figure, the peak/null values are somewhat under/over represented due to the 500-MHz sweep resolution used.

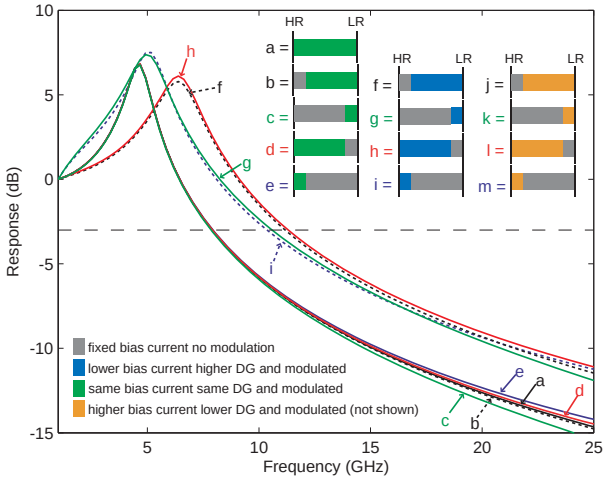

Fig. 3. Simulated modulation response of a 400-μm two-section laser under a variety of configurations identified in the legend (bottom left) and the lookup table (top right). In the legend, DG is an abbreviation for differential gain. The four cases, whose data is not shown, correspond to the so-called "inverted" gain lever which offers a reduced efficiency and lower resonance peak than the the other cases explored here. This data was omitted only to simplify the appearance of Figs. 3 and 4. The laser is split into a short (80 μm) and long (320 μm) section in this simulation. In this figure nine of the thirteen different ways a two-section laser of fixed section length but variable location and biasing is investigated.

The origin of the sharp dips is also physically intuitive; it is due to photons passing through the modulated section at its peak during one round trip only to pass through this section at its minimum during the following round trip. This situation is responsible for the nulls in the modulation response seen around 18, 27, 53, and 88 GHz. If the modulated sections were infinitesimally thin these features would all occur at $(n + 1/2)\times FSR_{laser}$ where n = 0,1..., however, because of the finite thickness of the modulated sections the dips are shifted to the locations reported in Fig. 4(b,c,f,g). This results in the nulls at 18 and 27 GHz being shared by only two curves, whereas the resonant peaks are shared by all but the single-section modulation case. The existence of the dips themselves, on the other hand, is related to the output facet used in the simulation. For example, in Fig. 4(c) by placing a modulated 250-μm section in front of the LR mirror it is found that a dip is created at the LR facet at 18 GHz. However, if the output was taken at the HR facet this null would not exist which is why no dip is found at these frequencies in Fig. 4(e). It can therefore be concluded that while the asymmetric cavity losses play a role in determining the strength of the modulation response, they do not affect the physics leading to the nulls themselves; it is due only to the modulation washing itself out. This same effect occurs at higher harmonics of the cavity (i.e. 18 GHz + $n\times FSR_{laser}$) although the situation is more complex for Fig. 4(b) and (d) which is why a null is not found at 60 GHz. In this case, a null is formed within the cavity at these frequencies but they are amplified to the levels reported in this figure before reaching the facet.

Nulls are also formed by the finite transit time of the light in the section modulated [55]. In this case photons enter the modulated section at one extreme of the modulation cycle only to exit that section at the other modulation extreme causing the effect of the modulation on those photons to wash out on a timescale related to the length of the modulated section. The physical mechanism here is essentially the same as that which creates the other dips just commented on, it just occurs on a different time scale. This is a real issue, problematic for high-frequency modulators, which serves as the motivation for building traveling-wave modulators where the modulating RF signal propagates at the same speed as the light along the length of the structure [55, 56]. In these simulations the transit-time limitation leads to the dips at 40 and 80 GHz [the free-spectral range associated with the 1.0-mm section ($FSR_{section}$) and its higher harmonics]. Therefore by placing a modulated 1-mm section in front of the HR mirror, in Fig. 4(d), it is found that a dip is created

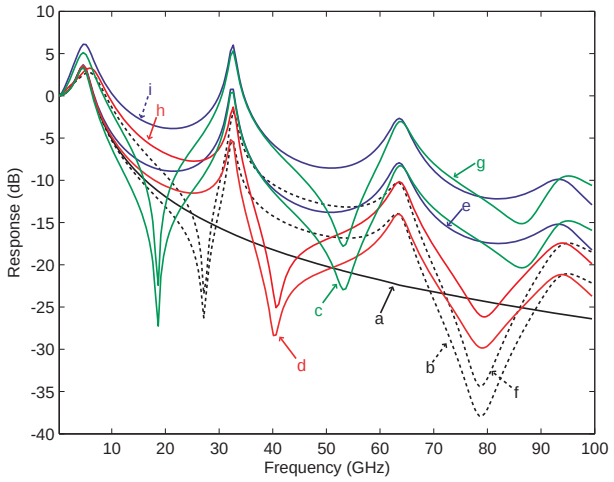

Fig. 4. Simulated modulation response of a 1.25-mm two-section laser under a variety of configurations identified by the legend (bottom left) and the lookup table (top right) in Fig. 3. The laser was split into a short (250 μm) and long (1 mm) section in this simulation. In this figure, nine of the thirteen different ways a two-section laser of fixed section length but variable location and biasing are investigated.

at the LR facet at 40 GHz and its harmonics. However, if the output was taken at the HR facet this dip would only exist at 80 GHz and its harmonics. This is why this effect only occurs for the single-pass frequencies $2\times n\times FSR_{section}$, where n = 1,2... in Fig. 4(b). Of course because the $FSR_{section}$ of the 250-μm section is 160 GHz this effect plays no role in Fig. 4(c,e,g,i) over the frequency range explored.

Regardless of their origin, these dips may be difficult to identify experimentally due to signal-to-noise ratio issues especially when the device impedance is not properly matched and the modulation is accompanied by a parasitic capacitance. In this case, the higher frequency components will be driven into the noise floor of the test equipment obscuring the presence of any dips which may be present.

A useful finding made by careful inspection of Fig. 4 is that even for modulation studies well below the laser's FSR_{laser} (say up to 15 GHz here) spatial effects will change the modulation response making it difficult to obtain accurate fits with the gain-lever model at higher frequencies [47] or leading experimentalists to improperly fit their results with the gain-lever model thus erroneously extracting lifetimes. Finally, the single-section response shown in Fig. 4(a) mandates explanation. Regardless of the device structure, the physical effect of resonant modulation is always present and so one might expect these structures to also display a peak. Nevertheless, for devices with identical facet reflectivity's, the finite transit time's filtering effect exactly cancels this out and the result predicted by the most basic model for single-section modulation [50] still holds true.

5. CONCLUSIONS

An overview of multi-section semiconductor lasers, external-cavity semiconductor lasers, and the modulation of semiconductor lasers was reported in order to highlight that spatial effects in these devices have not been sufficiently investigated. The gain-lever model was reproduced because of the focus on multi-section devices, and it was compared with the modulation from a single-section device. This model reveals the well-known results that the modulation bandwidth and/or efficiency can be improved by using a multi-section device. Numerical simulations based on a traveling-intensity equation model were used to incorporate spatial effects and investigate the gain-lever effect when the spatial dimension of the device plays a role. The findings indicate that at high frequencies or for long cavity lengths feedback enhancement causes the modulation response to depart from that predicted using analytic results. This not

only occurs near the FSR but at frequencies substantially removed from it as well. Finally, our simulations predict not only resonant peaks in the modulation response but also dips due to transit time limitations.

ACKNOWLEDGEMENTS

N. Usechak, M. Grupen, and V. Kovanis were supported by AFOSR LRIR 09RY04COR. N. Naderi, Y. Li, and L. Lester acknowledge the support of AFRL FA8750-06-1-0085. The support of the Air Force does not constitute an endorsement by the U.S. Government of the views or opinions expressed herein.

*

REFERENCES

[1] B. S. Goldstein and R. M. Weigand, "X-band modulation of GaAs lasers," *Proc. IEEE (Correspondence)*, 53, 195–196 (1965).
[2] G. J. Lasher, "Analysis of a proposed bistable injection laser," *Solid State Electron.*, 7, 707–716 (1964).
[3] A. Kawaji, "Some properties of junction triode laser," *Jap. J. Appl. Phys.*, 3, 425–426 (1964).
[4] C. E. Kelly, "Interactions between closely coupled GaAs injection lasers," *IEEE Trans. Electron Dev.*, 12, 1–4 (1964).
[5] M. I. Nathan, J. C. Marcinace, R. F. Rutz, A. E. Michel, and G. J. Lasher, "GaAs injection laser with novel mode control and switching properties," *J. Appl. Phys.*, 36, 473–480 (1965).
[6] N. G. Basov, "Dynamics of injection lasers," *IEEE J. Quantum Electron.*, QE-4, 855–864 (1968).
[7] T.-P. Lee and R. H. R. Roldan, "Repetitively Q-switched light pulses from GaAs injection lasers with tandem double-section stripe geometry," *IEEE J. Quantum Electron.*, QE-6, 339–352 (1970).
[8] V. N. Morozov, V. V. Nikitin, and A. A. Sheronov, "Self-synchoronization of modes in a GaAs semiconducor injection laser," *JETP Lett.*, 7, pp. 256–258 (1968).
[9] K. Y. Lau, I. Ury, and A. Yariv, "Passive and active mode locking of a semiconductor laser without an external cavity," *Appl. Phys. Lett.*, 46, 1117–1119 (1985).
[10] J. W. Crow and J. R. M. Craig, "GaAs laser linewidth measurmetns by hetrodyne detection," *Appl. Phys. Lett.*, 5, 72–74 (1964).
[11] L. A. Glasser, "C.W. modelocking of a GaAlAs laser diode," *Electron. Lett.*, 14, 725–726 (1978).
[12] K. Kobayashi, "Improvements in direct pulse code modulation of semiconductor lasers by optical feedback," *Trans. IECE Japan*, E59, 8–14 (1976).
[13] R. P. Salathé, "Diode lasers coupled to external resonators," *Appl. Phys.*, 20, 1–18 (1979).
[14] R. Lang and K. Kobayashi, "External optical feedback effects on semiconductor injection laser properties," *IEEE J. Quantum Electron.*, QE-16, 347-355 (1980).
[15] R. Lang, "Injection locking properties of a semiconductor laser," *IEEE J. Quantum Electron.*, QE-18, 976–983 (1982).
[16] G. J. Aspin and J. E. Carroll, "Simplified theory for mode locking in injection lasers," *IEE J. Solid-State & Electron Devices*, 3, 220–223 (1979).
[17] H. A. Haus, "Models of modelocking a laser diode in an external resonator," *IEE Proc.*, 127, 323–329 (1980).
[18] L. A. Glasser, "A linearized theory for the diode laser in an external cavity," *IEEE J. Quantum Electron.*, QE-16, 525–531 (1980).
[19] K. Y. Lau and A. Yariv, "Direct modulaton and active mode locking of ultrahigh speed GaAlAs lasers at frequencies up to 18 GHz," *Appl. Phys. Lett.*, 46, 326–328 (1985).
[20] G. P. Agrawal, "Generalized rate equations and modulation characteristics of exteranl-cavity semiconductor lasers," *J. Appl. Phys.*, 56, 3110–3115 (1984).
[21] G. P. Agrawal and C. H. Henry, "Modulation performace of a semiconductor laser coupled to an external high-Q resonator," *IEEE J. Quantum Electron.*, 24, 134–142 (1988).
[22] K. Y. Lau, N. Bar-Chaim, I. Ury, and A. Yariv, "11-GHz direct modulation bandwidth GaAlAs window laser on semi-insulationg substrate operating at room temperature," *Appl. Phys. Lett.*, 45, 316–318 (1984).

[23] K. Y. Lau, "Efficient narrow-band direct modulation of semiconductor injection lasers at millimiter wave frequncies of 100 GHz and beyond," *Appl. Phys. Lett.*, 52, 2214–2216 (1988).
[24] K. Y. Lau, "Narrow-band modulation of semiconductor lasers at millimeter wave frequencies (> 100 GHz) by mode locking," *IEEE J. Quantum Electron.*, 26, 250–261 (1990).
[25] K. Y. Lau and J. B. Georges, "On the characteristics of narrow-band resonant modulation of semiconductor lasers beyond relaxation oscillation frequency," *Appl. Phys. Lett.*, 63, 1459–1461 (1993).
[26] J. Helms and K. Petermann, "Microwave modulation of laser diodes with optical feedback," *IEEE J. Lightwave Technol.*, 9, 468–476 (1991).
[27] R. Nagarajan, S. Levy, A. Mar, and J. E. Bowers, "Resonantly enhanced semiconductor lasers for efficient transmission of millimeter wave modulated light," *IEEE Photon. Techn. Lett.*, 5, 4–6 (1993).
[28] K. Petermann, "External optical feedback phenomena in semiconductor lasers," *IEEE J. Sel. Top. Quantum Electron.*, 1, 480–489 (1995).
[29] G. P. Agrawal, "Coupled-cavity semiconductor lasers under current modulation: Small-signal analysis," *IEEE J. Quantum Electron.*, QE-21, 255–263 (1985).
[30] K. J. Vahala, M. A. Newkirk, and T. R. Chen, "The optical gain lever: A novel gain mechanism in the direct modulation of quantum well semiconductor lasers," *Appl. Phys. Lett.*, 54, 2506–2508 (1989).
[31] N. Moore and K. Y. Lau, "Ultrahigh efficiency microwave signal transmission using tandem-contact single quantum well GaAlAs lasers," *Appl. Phys. Lett.*, 55, 936–938 (1989).
[32] K. Y. Lau, "Narrow linewidth, continuously tunable semiconductor lasers based on quantum well gain lever," *Appl. Phys. Lett.*, 59, 2216–2218 (1991).
[33] C. P. Seltzer, L. D. Westbrook, and H. J. Wickes, "Improved signal-to-noise ratio in gain-levered InGaAsP/InP MQW lasers," *Electron. Lett.*, 29, 230–231 (1993).
[34] L. D. Westbrook and C. P. Seltzer, "Reduced intermodulation-free dynamic range in gain-lever lasers," *Electron. Lett.*, 29, 488–489 (1993).
[35] H. Olesen, J. I. Shim, M. Yamaguchi, and M. Kitamura, "Proposal of novel gain-levered MQW DFB lasers with high and red-shifted FM response," *IEEE Photon. Technol. Lett.*, 5, 599–602 (1993).
[36] D. McDonald and R. F. O'Dowd, "'inverted' gain-levered long-wavelength MQW optical transmitter with enhanced FM efficency and suppressed AM," *Electron. Lett.*, 30, 37–39 (1994).
[37] C. P. Seltzer, L. D. Westbrook, and H. J. Wickes, "The "gain-lever" effect in InGaAsP/InP multiple quantum well lasers," *IEEE J. Lightwave Technol.*, 13, 283–289 (1995).
[38] G. Griffel and C.-H. Chen, "Static and dynamic analysis of tunable two-section high-speed distrubuted feedback laser utilizing the gain lever effect," *IEEE J. Qunantum Electron.*, 32, 61–68 (1996).
[39] H.-K. Sung, T. Jung, D. Tishinin, K. Y. Liou, W. T. Tsang, and M. C. Wu, "Optical injection-locked gain-lever distributed Bragg reflector lasers with enhanced RF performance," *IEEE International Topical Meeting on Microwave Photonics*, MWP'04, 225–228 (2004).
[40] J. Klamkin, J. M. Hutchinson, J. T. Getty, L. A. Johansson, E. J. Skogen, and L. A. Coldren, "High efficiency widely tunable SGDBR lasers for improved direct modulation performance," *IEEE J. Sel. Top. Quantum Electron.*, 11, 931–938 (2005).
[41] M. Pocha, T. Bond, R. Welty, S. Vernon, J. Kallman, and E. Behymer, "Gain lever characterization in monolithically integrated diode lasers," *Proc. SPIE* 5722, 288–298 (2005).
[42] H.-K. Sung and M. C. Wu, "Amplitude modulation response and linearity improvement of directly modulatied lasers using ultra-strong injection-locked gain-lever distributed Bragg reflector lasers," *J. Optical Soc. of Korea*, 12, 303–308 (2005).
[43] A. Markus, M. Rossetti, V. Calligari, D. Chek-Al-Kar, J. X. Chen, A. Fiore, and R. Scollo, "Two-state switching and dynamics in quantum dot two-section lasers," *J. Appl. Phys.*, 100, 113–117 (2006).
[44] M. Pocha, L. L. Goddard, T. C. Bond, R. J. Nikolić, S. P. Vernon, J. S. Kallman, and E. M. Behymer, "Electrical and optical gain lever effects in InGaAs double quantum-well diode lasers," *IEEE J. Quantum Electron.*, 43, 860–868 (2007).
[45] F. Rana, C. Manolatou, and M. F. Schubert, "Tapered cavities for high-modulation-efficiency and low-distortion semiconductor lasers," *IEEE J. Quantum Electron.*, 43, 1083–1087 (2007).

[46] M. Radziunas, A. Glitzky, U. Bandelow, M. W. an U. Troppenz, J. Kreissl, and W. Rehbein, "Improving the modulation bandwidth in semiconductor lasers by passive feedback," *IEEE J. Quantum Electron.*, 13, 136–142 (2007).
[47] Y. Li, N. A. Naderi, V. Kovanis, and L. F. Lester, "Enhancing the 3-dB bandwidth via the gain-lever effect in quantum-dot lasers," *IEEE Photon. J.*, 2, 321–329 (2010).
[48] Y.-C. Xin, V. Kovanis, A. L. Gray, L. Zhang, and L. F. Lester, "Reconfigurable quantum dot monolithic multisection passive mode-locked lasers," *Optics Express*, 15, 7623–7633 (2007).
[49] Y. Li, F. L. Chiragh, Y.-C. Xin, C.-Y. Lin, J. Kim, C. G. Christodoulou, and L. F. Lester, "Harmonic mode-locking using the double interval technique in quantum dot lasers," *Opt. Express*, 18, 14637–14643 (2010).
[50] S. L. Chuang, [Physics of Optoelectronic Devices] New York: John Wiley & Sons (1995).
[51] P. Vasil'ev, "High-power high-frequency picosecond pulse generation by passively Q-switched 1.55 μm diode lasers," *IEEE J. Quantum Electron.*, 29, 1687–1692 (1993).
[52] S. Bischoff, "Modeling colliding-pulse mode-locked semiconductor lasers," Ph.D. dissertation, Technical University of Denmark, Lyngby (1997).
[53] P. D. Yoder, M. Grupen, and R. K. Smith, "Demonstration of intrinsic tristability in double-barrier resonant tunneling diodes with the Wigner transport equation," *IEEE Trans. Electron Dev.*, 57, 3265–3274 (2010).
[54] M. Grupen and K. Hess, "Simulation of carrier transport and nonlinearities in quantum-well laser diodes," *IEEE J. Quantum Electron.*, 34, 120–140 (1998).
[55] A. Yariv, [Quantum Electronics], 3rd ed. New York: John Wiley & Sons (1987).
[56] S. Shi and D. W. Prather, "Dual rf-optical slot waveguide for ultrabroadband modulation with a subvolt V_π," *Appl. Phys. Lett.*, 96, 201107–201109 (2010).